Revista Virtual de Química
ISSN 1984-6835

Artigo

Understanding the Solid Forms of 5*E*-phenylethenylbenzofuroxan with Different *in vivo* anti-*T. cruzi* Activity

Honorato, S. B.; Porcal, W.; Merlino, A.; Ellena, J.; Cerecetto, H.; A. P., Ayala*, González, M.*

Rev. Virtual Quim., **2013**, *5* (6), 1179-1190. Data de publicação na Web: 6 de novembro de 2013

http://www.uff.br/rvq

Compreendendo as Formas Sólidas de 5*E*-(feniletenil)benzofuroxano com Diferente Atividade anti-*T. cruzi in vivo*

Resumo: 5*E*-(feniletenil)benzofuroxano (**5PhEBfx**) foi descrito como um excelente candidato a fármaco anti-chagásico. Entretanto, sua biodisponibilidade oral foi afetada pelo processo de cristalização. Duas amostras exibindo variável atividade *in vivo* foram investigadas: um pó fino amarelo (**5PhEBfx-Y**) e agulhas laranjas (**5PhEBfx-O**). Difração de raios X de pó, calorimetria exploratória diferencial, espectroscopia vibracional, microscopia óptica e eletrônica de varredura foram aplicados para investigar as duas formas sólidas a fim de correlacionar as propriedades do estado sólido do composto **5PhEBfx** com sua variável biodisponibilidade. Foi observado que o **5PhEBfx-Y** tem uma melhor solubilidade e, consequentemente, maior biodisponibilidade quando comparado com o **5PhEBfx-O**. Este resultado sugere que a diferença de atividade entre estes dois arranjos em estado sólido do 5*E*-(feniletenil)benzofuroxano poderia estar associada a perfil de biodisponibilidade distinto e a variação de coloração do composto.

Palavras-chave: Formas sólidas; 5*E*-(feniletenil)benzofuroxano; agentes anti-*T. Cruzi*; solubilidade; biodisponibilidade.

Abstract

5*E*-Phenylethenylbenzofuroxan (**5PhEBfx**) was reported as an excellent anti-Chagas drug candidate. However, its oral bioavailability was affected by the crystallization process. Two samples exhibiting variable *in vivo* activity was investigated: a thin yellow powder (**5PhEBfx-Y**) and orange needles (**5PhEBfx-O**). X-ray powder diffraction, differential scanning calorimetry, vibrational spectroscopy, optical and electron scanning microscopies were applied to investigate both solid forms in order to correlate the solid-state properties with the variable bioavailability of **5PhEBfx**. It was observed that **5PhEBfx-Y** have a better solubility and consequently higher bioavailability when compared with **5PhEBfx-O**. This result suggests that the difference of activity between these two 5*E*-Phenylethenylbenzofuroxanes could be associated with the solid forms, which also cause the coloration variation.

Keywords: Solid forms; 5*E*-Phenylethenylbenzofuroxan; anti-*T. cruzi* agents; solubility; bioavailability.

* Universidad de la República, Laboratorio de Química Orgánica, Facultad de Ciencias, Iguá 4225, 11400, Montevideo, Uruguay. Tel./Fax: 5982 5250749.
megonzal@fq.edu.uy

Volume 5, Número 6 Novembro-Dezembro 2013

Revista Virtual de Química
ISSN 1984-6835

Understanding the Solid Forms of 5*E*-phenylethenylbenzofuroxan with Different *in vivo* anti-*T. cruzi* Activity

Sara B. Honorato,[a] Williams Porcal,[b] Alicia Merlino,[b] Javier Ellena,[c] Hugo Cerecetto,[b,d] Alejandro P. Ayala,[a] Mercedes González[b,*]

[a] Universidade Federal do Ceará, Departamento de Física, CP 6030, CEP 60.455-760, Fortaleza-CE, Brasil.

[b] Universidad de la República, Grupo de Química Medicinal, Laboratorio de Química Orgánica, Facultad de Química-Facultad de Ciencias, Iguá 4225, Montevideo, 11400, Uruguay.

[c] Universidade de São Paulo, Instituto de Física de São Carlos, CP 369, CEP 13560-970, São Carlos-SP, Brazil

[d] Universidad de la República, Current address: Área de Radiofarmacia, Centro de Investigaciones Nucleares, Facultad de Ciencias, Mataojo 2055, 11400 Montevideo, Uruguay

* megonzal@fq.edu.uy

Recebido em 17 de setembro de 2013. Aceito para publicação em 5 de novembro de 2013

1. Introduction

5*E*-Phenylethenylbenzofuroxan (**5PhEBfx**, Figure 1) is currently in pre-clinical studies as anti-Chagas drug candidate.[1-4] Chagas disease or American trypanosomiasis is an important health problem that affects around twenty million people in Central and South America. Around 2–3 million individuals develop the typical symptoms of this disease that results in 50,000 deaths yearly.[5-7] Due to the current pharmacology for this illness is still inefficient[8,9] we have been investigating during the last fifteen years, the development of new drugs.[10] **5PhEBfx** was initially studied as a thin yellow powder (**5PhEBfx-Y**) during the initial development steps finding excellent *in vitro*[11] and *in vivo* activities.[3]

However, during the pre-clinical studies **5PhEBfx** was purified by successive crystallizations[1,2] giving rise to an orange crystalline form (**5PhEBfx-O**) finding that its *in vivo* biological properties changed. In this last case, the compound, in its orange crystalline form, became less active *in vivo* than the previous solid form used in the initial studies (*i.e.* yellow powder material, **5PhEBfx-Y**)[3] (Figure 2). These different findings could be the result of the increased solubility of **5PhEBfx-Y**, and thus its bioavailability, and may suggest the existence of polymorphism.

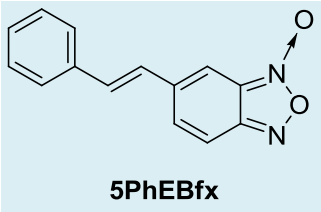

Figure 1. Structural formula of benzofuroxan with anti-*T. cruzi* activity

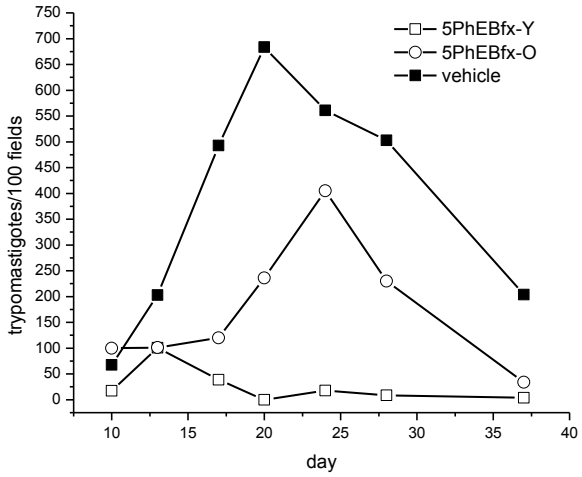

Figure 2. Effects of the different studied solid forms of **5PhEBfx** on parasitemia in the murine model of acute Chagas disease following experimental conditions of ref. (3)

Briefly, **5PhEBfx-Y** and **5PhEBfx-O** were suspended in the vehicle (saline: tween 80, 4:1) immediately prior to used, no more than 30 min before the administration, and the formulation was orally administered to the animals using intragastric syringe, on a daily

basis, during 25 days beginning day five post-infection (with the Tulahuen 2 strain of *T. cruzi*) (the experimental protocol with animals was approved by the Animal Ethics Committee of the Universidad Nacional de Rosario). The effect of each solid form, or vehicle (without treatment), was weekly evaluated by determining the blood trypomastigotes levels.[12] The groups were represented by untreated animals (vehicle) and those receiving **5PhEBfx-Y** (yellow powder form) and **5PhEBfx-O** (orange crystalline form).[3]

Solid drugs can exist in different solid-state forms, such as crystalline, which comprise hydrates, solvates, salts and co-crystal, and amorphous forms, with different range of physicochemical properties, such as morphology, density, stability, melting point and solubility of the product. This can also affect the biological activity, for example differences in the bioactivity, as consequence of the drug bioavailability.[13,14] Usually, a pharmaceutical solid is manufactured in a stable crystalline form because the amorphous form could tend to convert to the crystalline form due to its thermodynamic potential instability. This avoid the possible interchangeable between the amorphous and crystalline form in lifetime. However, despite this possible disadvantage, the amorphous state has attracted considerable interest in the formulation of poorly soluble compounds. The higher molecular mobility of this material, for instance, may improve the solubility and dissolution rate of the pharmaceutical solid and, thus, facilitate the gastrointestinal absorption of the active components.[15,16]

Several authors reported the effects of the solid-state properties of a drug on its biopharmaceutical properties.[14,17,18] These effects could be originated at different levels. At a supramolecular level, the crystal packing of the drug molecules could give rise to different polymorphs, which could exhibit variable solubility. Given a crystalline form, the thermodynamic conditions of the preparation process could originate changes in the crystalline habit. Changes in the solid-state properties are usually reflected in diverse microscopic and macroscopic physicochemical properties, like melting point, crystalline habit or color. A very well known example of the effect of polymorphism in the macroscopic properties is 5-methyl-2-[(2-nitrophenyl)amino]-3-thiophenecarbonitrile, which has been crystallized in seven polymorphs varying color and crystalline habit. The system has been named ROY for its red, orange, and yellow crystal colors.[20] Thus, not only the crystalline habit but also the sample color could be indicative of structural changes in the solid form. Combining these evidences with the variable bioavailability observed in the **5PhEBfx** samples, one might propose that the solid-state properties are playing a relevant role in the oral *in vivo* activity of this drug. As a consequence, the aim of this work is to correlate the biopharmaceutical results of **5PhEBfx** with its solid-state properties. Modified materials properties were investigated by solubility at two different conditions (aqueous solutions at stomach- and intestine-like pHs), melting point, optical and scanning electron (SEM) microscopies, Fourier-transform infrared and Raman spectroscopy, differential scanning calorimetry (DSC) and X-ray powder diffraction (XRPD).

2. Experimental

2.1. Chemicals

Compound **5PhEBfx** was obtained in our laboratory according to previously published methods.[1] The samples homogeneity was achieved by NMR spectroscopy and microanalysis. All reagents and chemicals were of analytical grade. Other reagents were analytical grade and double distilled water was used throughout the experiment. For animal studies, Milli-Q water purified using Millipore system was used.

2.2. Preparation of solid forms

Crystalline form of studied compound, **5PhEBfx-O**, was obtained by crystallization from petroleum ether:EtOAc. It was prepared by cooling a boiling petroleum ether:EtOAc (85:15, v/v) solution (near saturation) at room temperature. Amorphous material, **5PhEBfx-Y**, was prepared by dissolution in an appropriate amount of a mixture of petroleum ether:EtOAc (70:30, v/v) follow by solvent evaporation under vacuum, at room temperature in a rotary evaporator, and ground in a mortar. Both **5PhEBfx** were obtained with purity major to 99 %. The solid materials were stored in closed glass vials.

2.3. Analytical techniques

2.3.1. Relative solubility of solid forms

The relative solubility of **5PhEBfx-O** and **5PhEBfx-Y** were determined in triplicate using a modified shake-flask method.[21,22] Two different conditions were used, aqueous solutions at pH=2.0 like rat stomach condition and pH=5.0 like proximal small intestine in the fed state condition.[23] The aqueous solution at different pHs were obtained with non-phosphate buffers. Increasing amounts of the studied solid were added to the corresponding buffer solution and incubated during 30 min. Then, the solutions were filtered and the compound amount was quantified by UV spectroscopy at 300 nm.

2.3.2. X-ray powder diffraction

The XRPD patterns were recorded on X-ray diffractometer (PW 1729, Philips, The Netherlands). Samples were irradiated with monochromatized Cu-Ka radiation (1.542Å) and analyzed from 5^{o} to 50^{o} 2θ. The voltage and current used were 30 kV and 30 mA, respectively.

2.3.3. Differential scanning calorimetry

Thermograms were recorded using a Netzsch Phoenix 204 system (Netzsch, Germany). Duplicate samples of 1–3 mg were accurately weighed in sealed and pierced aluminium pans. Samples of each compound were heated from room temperature to approximately 50 ^{o}C above the melting temperature at a rate of 5 ^{o}C min^{-1} under nitrogen at a flow rate of 60 mL min^{-1}.

2.3.4. Vibrational spectroscopy

Infrared spectra were recorded on a Bruker Vertex 70 Fourier transform spectrometer (Bruker Optik, Ettlingen, Germany). The spectrometer was equipped with a KBr beamsplitter, an MIR source and a RT-DLaTGS detector. Samples were measured over a wavelength range from 400 to 4000 cm^{-1} and the final spectrum was the mean of 128 scans. A RAM II module was employed to obtain the Raman spectra in the spectral range between 80 and 3600 cm^{-1} using a diode pumped Nd:YAG laser with an excitation wavelength of 1064 nm at a laser power of 100 mW. Each spectrum was the average of 512 scans.

2.3.5. Microscopy

The morphology of **5PhEBfx-O** and **5PhEBfx-Y** were studied by optical microscopy and scanning electron microscope (SEM). The SEM was utilized to assess the morphological characteristics of the row materials and the drug–carrier systems using a Tescan Model XMU, VEGA II. The samples were fixed on aluminum stubs with double-sided tape, 15 nm gold coated sputter and examined in the microscope using an accelerating voltage of 30 kV, at a working distance of 8 mm.

3. Results

3.1 Relative solubility of solid forms

The relative solubility of the solid materials was assessed, using UV measurement, in two different conditions corresponding to the biological absorption-pHs (Table 1, Figure 3). In the experimental conditions neither **5PhEBfx-O** nor **5PhEBfx-Y** achieved visually complete dissolution at the acidic pH (pH= 2). This observation was confirmed by the UV studies. The **5PhEBfx-Y** showed relevant solubility-enhancement in the intestine-like pH (pH= 5).

3.2. X-ray powder diffraction

As it was previously stated, the studied solid forms exhibit distinctive colours as shown in Figure 4. In order to investigate the crystalline structure of the two samples of **5PhEBfx** X-ray powder diffraction (XRPD) measurements were performed. These results are presented in Figure 5 compared with the simulated pattern calculated from the crystalline structure of **5PhEBfx**. X-ray single crystal measurements in **5PhEBfx-O** allowed us to determine its crystalline structure.[24] **5PhEBfx-O** crystallizes in an orthorhombic lattice belonging to the P212121 space group (a = 7.2368(6) Å, b = 12.613(1) Å and c = 12.884(1) Å). The solid-state packing of this compound is based on two contacted infinite one-dimensional chains parallel to [001] direction and they are related by a 21 screw axis symmetry along the c axis. Into each chain, the molecules are connected along the packing direction through a C–H…O weak intermolecular interaction, in a head-to-tail array, whereas each benzofuroxan is bonded to other two molecules from an adjacent chain through another weak non-classical intermolecular hydrogen bonding involving C–H…O, in a zigzag manner.

Table 1. Relative solubility ($S_{5PhEBfx-Y}/S_{5PhEBfx-O}$) of the solid forms in different conditions

Condition	$S_{5PhEBfx-Y}/S_{5PhEBfx-O}$
pH=2.0	both forms are completely insoluble in the assayed conditions
pH=5.0	1.5

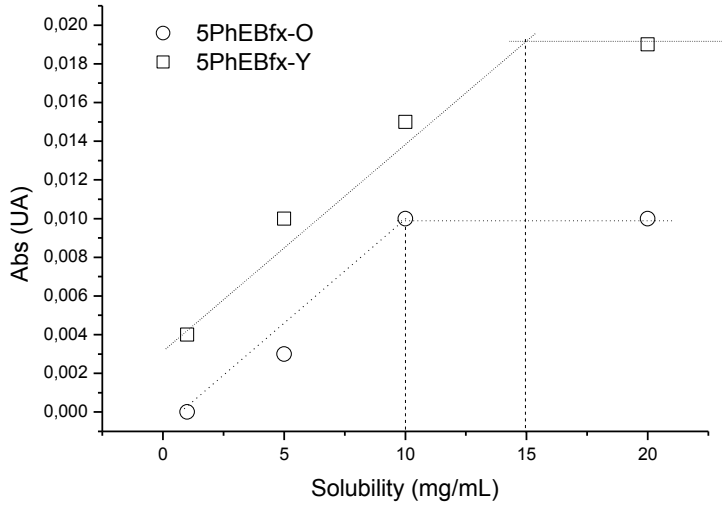

Figure 3. Example of UV-behavior of the solid materials of the **5PhEBfx-O** and **5PhEBfx-Y** at pH=5.0.

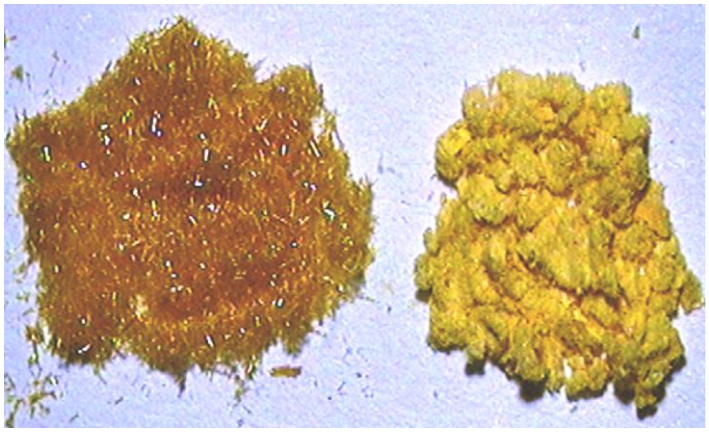

Figure 4. Photograph of **5PhEBfx:** orange needles (left, **5PhEBfx-O**) and yellow powder (right, **5PhEBfx-Y**)

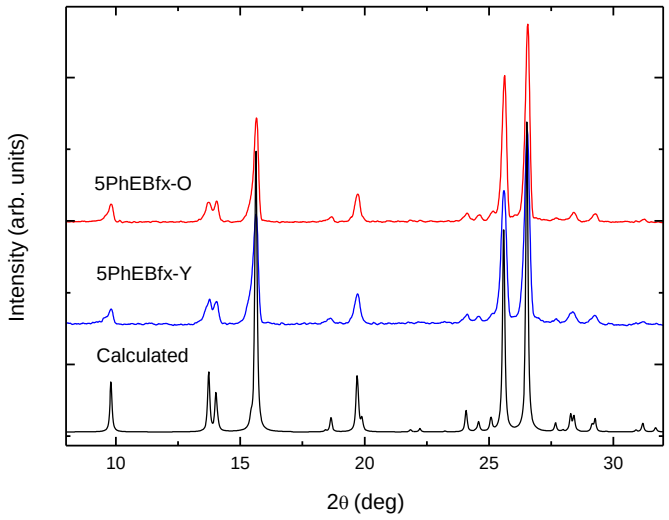

Figure 5. Comparison between the X-ray powder patterns simulated from the **5PhEBfx** crystal structure (vertical bars) and experimental patterns of the **5PhEBfx-Y** and **5PhEBfx-O** at room temperature

3.3. Differential scanning calorimetry

The thermal stability of **5PhEBfx** was investigated by differential scanning calorimetry (DSC). The thermograms of both forms are presented in Figure 6. A typical curve is characterized by a sharp endothermic event (onset: 144.9°C; ΔH = 126.6 J/g) followed by a wide exothermic event (onset: 150°C; ΔH = -966.9 J/g). The first event is related to the melting of the compound, which is followed by its decomposition (exothermic event).

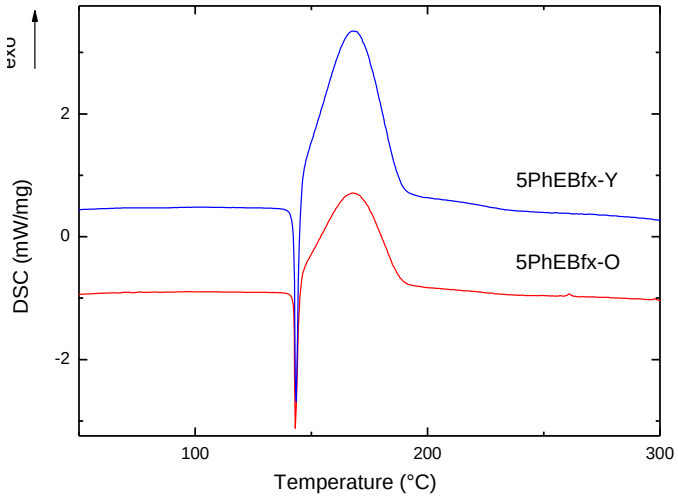

Figure 6. DSC curves for **5PhEBfx-O** and **5PhEBfx-Y**

3.4. Vibrational spectroscopy

Raman and infrared spectra of the investigated samples are presented in Figure 7. As it was observed in XRPD and DSC measurements, no evidences of structural modifications were found in the vibrational spectra of **5PhEBfx**. Due to that, just representative spectra of this compound are shown in Figure 7. The Raman spectrum of **5PhEBfx** was previously discussed,[24] where quantum mechanical calculations were used to assign the most relevant vibrational modes. These calculations produced a very good agreement between the experimental and theoretical results and allow us to also apply them to interpretation of the infrared spectrum.

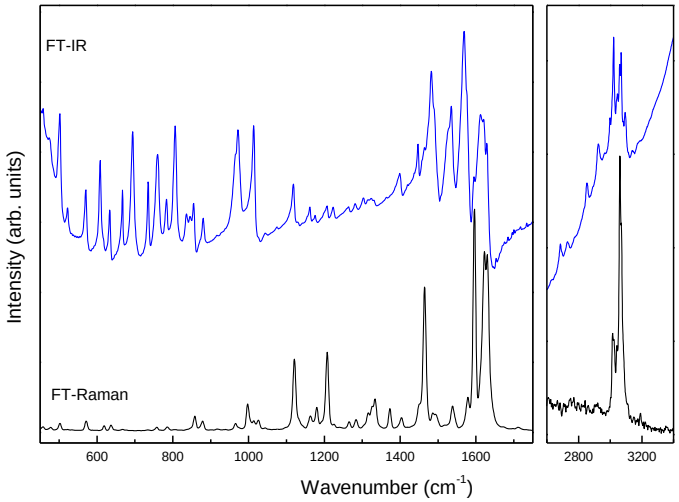

Figure 7. Raman and infrared spectra of **5PhEBfx**.

3.5. Scanning electron microscopy

Figure 8 shows the SEM images recorded from **5PhEBfx-O** and **5PhEBfx-Y** samples. From these images, one can observe that both samples exhibit the same acicular crystalline habit. However, **5PhEBfx-O** exhibits bigger crystals of around 100 ?m, whereas a smaller particle size (around 50??m) is observed in **5PhEBfx-Y**.

4. Discussion

According to the solubility studies performed, it could point out that both samples are insoluble in the simulated gastric pH conditions whereas it increases considerably in the intestine pH conditions (pH 5.0). Being the maximum solubility for **5PhEBfx-Y** 15 mg/mL and for **5PhEBfx-O** 10 mg/mL. This increase in solubilization was attributed initially to amorphization of **5PhEBfx**. This information allows us to hypothesize that the studied solid forms would penetrate *in vivo* mainly in the rat proximal small intestine (Table I, Figure 3). After this supposition, we investigated whether these two samples have differential solid properties to be considered two different solid forms. The X-ray studies were performed in powder and crystalline form of the all the samples. The comparison between the experimental and simulated patterns of **5PhEBfx-O** confirms that the raw material is in the same crystalline structure that the measured single crystal. It is an expected result, but comparing **5PhEBfx-O** and **5PhEBfx-Y** one may notice that both samples exhibit the same diffraction pattern. It is also important to point out that no evidence of an

amorphous phase is observed in X-ray powder diffraction. Thus, this experimental technique is not supporting the assumption that the variable solubility of the **5PhEBfx** samples is associated to polymorphism. Moreover, by comparing the DSC thermograms of **5PhEBfx-O** and **5PhEBfx-Y** the same events can be identified in both samples. The vibrational spectral studies of **5PhEBfx-O** and **5PhEBfx-Y** also indicated the total superposition of both samples. Based on the quantum mechanical calculations and the comparison with similar molecules the main features of the vibrational spectra were identified. Thus, the CC stretching bands of mono-substituted benzene are observed at 1450, 1496, 1578, and 1595 cm^{-1}. In the infrared spectrum the phenyl ring breathing modes are well visible at 785 cm^{-1} and 761 cm^{-1}, with contribution of the deformation modes δ(NO) from benzofuroxan. The C-H in-phase bend is assigned at 1334 cm^{-1} and 1315 cm^{-1} in the Raman spectrum. The C-H in-plane bendings of the phenyl ring are observed at 1181 cm^{-1} and 1076 cm^{-1}. Trigonal C-C-C bending mode of the phenyl group corresponds to the band at 1014 cm^{-1}. In the infrared spectrum, the C-H out-of-plane trigonal vibrations of phenyl ring are better observed at 996 cm^{-1} and 973 cm^{-1}, whereas the C-H out-of-plane modes are at 965, 918, and 879 cm^{-1}. In the Raman spectrum of **5PhEBfx**, two intense bands appear at 1630 cm^{-1} and 1621 cm^{-1}. The former is assigned to CC stretching modes of the benzofuroxan with apparent contributions of C-C stretching of ethenyl and CN stretching of benzofuroxan. The δ(C-H) modes of benzofuroxan are observed at 1403 cm^{-1}. Bands above 3000 cm^{-1} are assigned to the phenyl C-H stretching modes.

Several factors can modify the bioavailability of a drug and consequently its absorption. Some examples are the dissolution, pH in the absorption place, particle size, crystalline/amorphous forms of the drug, modifications in the chemical form and formulation adjuvants. In literature, several works emphasize the advantages of the use of amorphous pharmaceutical[25-27]. However, from the point of view of the thermodynamic stability, crystalline forms are still the best formulation option, due to the amorphous forms are instable and could go to crystalline ones. In this case, the dissolution rate of a drug, which is one of the most limiting properties affecting the bioavalability, is strongly influenced by the particle size. It is well known that the dissolution rate can be proportionally enhanced by increasing the surface area, which in turn increases with decreasing particle sizes.[28-33] This approach is frequently used in the pharmaceutical industry to deal with poorly soluble drugs by a micronization process.[30,34-36] Considering the variable solubility of the **5PhEBfx**, SEM results clearly show that the main difference between the two investigated samples is the particle size. Even the preliminary observations have suggested that the samples could exhibit different crystalline forms, the solid-state characterization ruled out this hypothesis. On the other hand, the variable particle size is not only supported by the microscopy observations. The DSC thermograms and X-ray powder diffraction patterns of the **5PhEBfx-Y** sample exhibits a slightly wider peaks which could be related to the smaller particle size. Thus, the increase in solubility of the **5PhEBfx-Y** was attributed to the different particle size of this form comparing to **5PhEBfx-O** increasing the effective surface area available for solubilization.

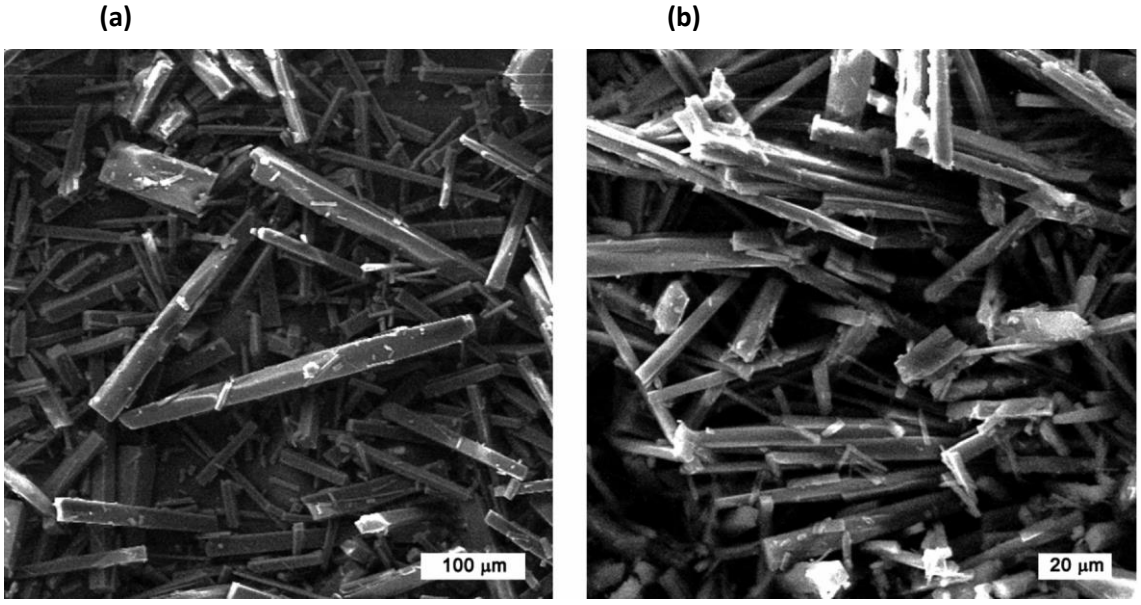

Figure 8. Photomicrographs of different crystal habits from **5PhEBfx-O (a)** and **5PhEBfx-Y (b)**

5. Conclusion

In this work, the solid-state properties of two samples of the anti-Chagas **5PhEBfx** with variable oral *in vivo* activity were compared. Our results suggest that the crystalline structure of the studied drug **5PhEBfx** was preserved during the crystallization processes. X-ray powder diffraction, vibrational spectroscopy and differential scanning calorimetry have confirmed that the two samples, despite the color differences, possess the same crystalline structure. Based on scanning electron microscopy and the X-ray powder diffraction we have inferred that the crystalline habit of the samples of **5PhEBfx** was the same, being differentiated only for the particle size. Our results show that the solubility of a drug can vary not only due to the polymorphism but also can be affected by the particle size, causing, thus, different *in vivo* activities.

Acknowledgements

The authors gratefully acknowledge CAPES, FINEP, IPDI and FUNCAP. This work was done as part of the project PROSUL-CNPq and the project "Clinical Development of Arylethenylbenzofuroxan Derivatives as Drugs for Chagas Disease" which received financial support from *Drugs for Neglected Diseases initiative*. The authors gratefully acknowledge Prof. Roland Bose from University of Duisburg-Essen for the X-ray powder diffraction measurements.

References

[1] Porcal, W.; Merlino, A.; Boiani, M.; Gerpe, A.; González, M.; Cerecetto, H. *Org. Proc. Res. Devel.* **2008**, *12*, 156. [CrossRef]

[2] Gerpe, A.; Merlino, A.; Boiani, M.; Porcal, W.; Fagiolino, P.; González, M.; Cerecetto, H. *J. Pharm. Biomed. Anal.* **2008**, *47*, 88. [CrossRef] [PubMed]

[3] Boiani, L.; Davies, C.; Arredondo, C.; Porcal, W.; Merlino, A.; Gerpe, A.; Boiani, M.; Pacheco, J.P.; Basombrío, M.A.; Cerecetto, H.; González, M. *Eur. J. Med. Chem.* **2008**, *43*, 2229. [CrossRef] [PubMed]

[4] Boiani, M.; Merlino, A.; Gerpe, A.; Porcal, W.; Croce, F.; DePaula, S.; Rodríguez, M.A.; Cerecetto, H.; González, M. *Xenobiotica*. **2009**, *39*, 236. [CrossRef] [PubMed]

[5] World Health Organization, available at <http://www.who.int/ctd/chagas> (accessed in November, 2013).
[6] Moncayo, A. In: World Health Organization. *Special Program for Research and Training in Tropical Diseases (TDR).* Geneva, 1993. p. 67. (Eleventh Programme Report of the UNPD).
[7] Urbina, J.A. *Curr. Pharm. Des*. **2002**, *8*, 287. [CrossRef] [PubMed]
[8] Cerecetto, H.; González, M. *Curr. Topics Med. Chem*. **2002**, *2*, 1185. [CrossRef] [PubMed]
[9] Cerecetto, H.; González, M. *Pharmaceuticals*, **2010**, *3*, 810. [CrossRef]
[10] Cerecetto, H.; González, M. *Mini. Rev. Med. Chem*., **2008**, *8*, 1355. [CrossRef] [PubMed]
[11] Aguirre, G.; Boiani, L.; Cerecetto, H.; Di Maio, R.; González, M.; Porcal, W.; Thomson, L.; Tórtora, V.; Denicola, A.; Möller, M. *Bioorg. Med. Chem.,* **2005**, *13*, 6324. [CrossRef] [PubMed]
[12] Cerecetto, H.; Di Maio, R.; González, M.; Risso, M.; Sagrera, G.; Seoane, G.; Denicola, A.; Peluffo, G.; Quijano, C.; Stoppani, A.O.M.; Paulino, M.; Olea-Azar, C.; Basombrío, M.A. *Eur. J. Med. Chem.* **2000**, *35*, 343. [CrossRef] [PubMed]
[13] Blagden, N.; de Matas, M.; Gavan, P.T.; York, P. *Adv. Drug. Delivery Rev.* **2007**, *59*, 617. [CrossRef] [PubMed]
[14] Huang, L.F.; Tong, W.Q. *Adv. Drug Delivery Rev*. **2004**, *56*, 321. [CrossRef] [PubMed]
[15] Yu, L. *Adv. Drug Delivery Rev*. **2001**, *48*, 27. [CrossRef] [PubMed]
[16] Hancock, B.C.; Zografi, G. *J. Pharm. Sci.* **1997**, *86*, 1. [CrossRef] [PubMed]
[17] Aaltonen, R.; Lewing, E.; Anttila, M.; Kristoffersson, E. *Intern. J. Pharm.* **1983**, *14*, 103. [CrossRef]
[18] Rasenack, N.; Muller, B.W. *Intern. J. Pharm*. **2002**, *245*, 9. [CrossRef] [PubMed]
[19] Ahlneck, C.; Zografi, G. *Intern. J. Pharm*. **1990**, *62,* 87. [CrossRef]
[20] Yu, L.; Stephenson, G.A.; Mitchell, C.A.; Bunnell, C.A.; Snorek, S.V.; Bowyer, J.J.; Borchardt, T.B.; Stowell, J.G.; Byrn, S.R.J. *J. Am. Chem. Soc.* **2000**, *122*, 585. [CrossRef]
[21] Fernández, L.; Calderón, M.; Martinelli, M.; Strumia, M.; Cerecetto, H.; González, M.; Silber, J.J.; Santo, M. *J. Phys. Org. Chem.* **2008**, *21*, 1079. [CrossRef]
[22] Wassvik, C.M.; Holmén, A.G.; Bergström, C.A.S.; Zamora, I.; Artursson, P. *Eur. J. Pharm. Sci.* **2006**, *29*, 294. [CrossRef] [PubMed]
[23] Bard, B.; Martel, S.; Carrupt, P.A. *Eur. J. Pharm. Sci*. **2008**, *33*, 230. [CrossRef] [PubMed]
[24] Martins, F.T.; Ayala, A.P.; Porcal, W.; Cerecetto, H.; González, M.; Ellena, J. *Mol. Diversity.* **2009**, 1381. [CrossRef] [PubMed]
[25] Murdande, S.B.; Pikal, M.J.; Shanker, R.M.; Bogner, R.H. *J. Pharm. Sci.* **2010**, *99*, 1254. [CrossRef] [PubMed]
[26] Lee, S.; Nam, K.; Kim, M.S.; Jun, S.W.; Park, J.S.; Woo, J.S.; Hwang, S.J. *Arch. Pharmacol. Res.* **2005**, *28*, 866. [CrossRef] [PubMed]
[27] Hancock, B.C.; Parks, M. *Pharm. Res.* **2000**, *17*, 397. [CrossRef] [PubMed]
[28] Johnson, K.C.; Swindell, A.C. *Pharm. Res.* **1996**, *13*, 1795. [CrossRef] [PubMed]
[29] Douroumis, D.; Fahr, A. *Eur. J. Pharm. Biopharm.* **2006,** *63*, 173. [CrossRef] [PubMed]
[30] Amidon, G.L.; Lennernäs, H.; Shah, V.P.; Crison, J.R. *Pharm. Res.* **1995**, *12*, 413. [CrossRef] [PubMed]
[31] Leuner, C.; Dressman, J. *Eur. J. Pharm. Biopharm*. **2000**, *50*, 47. [CrossRef] [PubMed]
[32] Chiou, W.L.; Riegelma, S. *J. Pharm. Sci.* **1971**, *69*, 1281. [CrossRef] [PubMed]
[33] Horter, D.; Dressman, J.B. *Adv. Drug Deliv. Rev.* **2001**, *46*, 75. [CrossRef]
[34] Liversidge, G.G.; Cundy, K.C. *Intern. J. Pharm.* **1995**, *125*, 91. [CrossRef]
[35] Jinno, J.; Kamada, N.; Miyake, M.; Yamada, K.; Mukai, T.; Odomi, M.; Toguchi, H.; Liversidge, G.G.; Higaki, K.; Kimura, T. *J. Controlled Release* **2006**, *111*, 56. [CrossRef] [PubMed]
[36] Dressman, J.B.; Reppas, C. *Eur. J. Pharm. Sci*. **2000**, *11*, S73. [CrossRef] [PubMed]